

THE ENERGY DEPENDENCE OF NEUTRON STAR SURFACE MODES AND X-RAY BURST OSCILLATIONS

ANTHONY L. PIRO

Department of Physics, Broida Hall, University of California
Santa Barbara, CA 93106; piro@physics.ucsb.edu

AND

LARS BILDSTEN

Kavli Institute for Theoretical Physics and Department of Physics, Kohn Hall, University of California
Santa Barbara, CA 93106; bildsten@kitp.ucsb.edu

Accepted for publication in The Astrophysical Journal

ABSTRACT

We calculate the photon energy dependence of the pulsed amplitude of neutron star (NS) surface modes. Simple approximations demonstrate that it depends most strongly on the bursting NS surface temperature. This result compares well with full integrations that include Doppler shifts from rotation and general relativistic corrections to photon propagation. We show that the energy dependence of type I X-ray burst oscillations agrees with that of a surface mode, lending further support to the hypothesis that they originate from surface waves. The energy dependence of the pulsed emission is rather insensitive to the NS inclination, mass and radius, or type of mode, thus hindering constraints on these parameters. We also show that, for this energy-amplitude relation, the majority of the signal (relative to the noise) comes in the $\approx 2\text{--}25$ keV band, so that the current burst oscillation searches with the *Rossi X-Ray Timing Explorer* are close to optimal. The critical test of the mode hypothesis for X-ray burst oscillations would be a measurement of the energy dependence of burst oscillations from an accreting millisecond pulsar.

Subject headings: stars: neutron — stars: oscillations — X-rays: bursts — X-rays: stars

1. INTRODUCTION

Accreting neutron stars (NSs) often show nearly coherent modulations during type I X-ray bursts (see reviews of Bildsten 1998; Strohmayer & Bildsten 2003) called burst oscillations (Muno et al. 2001, and references therein). The high temporal stability of each NS's characteristic frequency (within 1 part in 10^3 over years, Muno et al. 2002), along with burst oscillations seen from two accreting millisecond pulsars at their spin frequencies (Chakrabarty et al. 2003; Strohmayer et al. 2003) have led many to conclude that burst oscillations are a modulation at the NS spin frequency. Nevertheless, it has been a long standing mystery as to what creates the surface asymmetry in the burst tail, long after any hot spots from the burst ignition should have spread over the entire star (Bildsten 1995; Spitkovsky, Levin, & Ushomirsky 2002).

A recently developed and promising hypothesis is that burst oscillations are surface r -modes (Heyl 2004). In this picture the oscillations are created by a retrograde mode with an observed frequency just below the NS spin. As the star cools in the burst tail the mode replicates the observed rising frequency. Current theoretical work has focused on calculating the frequencies (Lee 2004; Piro & Bildsten 2005b) and flux perturbations (Heyl 2005; Lee & Strohmayer 2005) expected for such modes. Unfortunately, besides the highly sinusoidal nature of burst oscillations (Muno, Özel, & Chakrabarty 2002), which is expected for modes, there is little direct evidence that modes are the correct explanation. Piro & Bildsten (2005b) addressed this issue by calculating how the mode's properties would manifest themselves in the burst oscillations. First, they showed that higher persistent luminosity NSs should exhibit smaller frequency drifts, consistent with current observations. Second, they hypothesized that additional modes might be present with such large frequency drifts that they are difficult to detect. Though these are promising steps, both predictions

are directly tied to Piro & Bildsten's (2005b) model that the burst oscillations are a surface wave changing into a crustal interface wave (Piro & Bildsten 2005a). What is needed is a complementary, and more general, argument of how a surface mode should exhibit itself, independent of the specific model invoked. That is the goal of this present study.

A key characteristic of burst oscillations is a larger pulsed fraction at increasing energies in the range of $2\text{--}23$ keV (Muno, Özel, & Chakrabarty 2003, hereafter MOC03). This is distinct from other pulsing NSs. For example, accretion-powered millisecond X-ray pulsars decrease (marginally) in amplitude between $2\text{--}10$ keV (Cui, Morgan, & Titarchuk 1998; Galloway et al. 2002; Poutanen & Gierliński 2003). MOC03 modeled the burst oscillations as a hot spot on the NS surface and nicely reproduced the burst oscillation energy dependence. Given the promising possibility that the oscillation may be a mode, we perform a calculation of the pulsed amplitude as a function of energy for a nonradial oscillation. Similar studies have recently been completed by Heyl (2005) and Lee & Strohmayer (2005). Our work differs from these in that we are primarily interested in comparisons with observations, and thus do not perform an exhaustive parameter survey. We also include analytic estimates to explain our numerical calculations.

A primary difficulty with comparisons between theory and observations is that the mode amplitudes are not predicted from linear mode calculations. To overcome this complication we follow the example of pulsating white dwarf (WD) studies (Kepler et al. 2000) and only fit the *shape* of the energy dependence, leaving the overall amplitude as a free parameter. Unfortunately, bursting NSs have a drawback with respect to pulsating WDs in that the limb darkening of their bursting envelope is largely independent of photon energy above ≈ 1 keV (Madej 1991). This prevents constraining NS properties with burst oscillation data because the inclination, NS

mass, M , and radius, R , and even the mode's angular eigenfunction only alter the pulsed amplitude normalization as we show in §2.3. For this reason, full integrations of the pulsed NS emission are well replicated by an analytic result that only depends on the NS surface color temperature, T_c (eq. [8]).

We compare our result with the observed energy dependence of burst oscillations, finding agreement for $k_B T_c \approx 2-3$ keV, as expected for NSs during X-ray bursts. This suggests that the burst oscillations are due to a nonradial mode, independent of the mode's identification. The excitation and nonlinear evolution of the mode is of utmost importance if we are to infer NS attributes from burst oscillations.

In §2 we calculate the energy dependence of a mode's amplitude and compare it with X-ray burst oscillations in §3. In §4 we investigate the optimal photon energy ranges for detection of burst oscillations. We conclude in §5 with a summary of our results and note the importance of measuring the energy dependence of burst oscillations from an accreting millisecond pulsar.

2. THE ENERGY DEPENDENCE OF A MODE'S AMPLITUDE

We first describe our procedure for calculating the pulsed amplitude of a surface mode as a function of energy. This follows previous studies of pulsed NS emission (for example, Poutanen & Gierliński 2003), but is included to provide context for our analytic results in §2.2. In §2.3 we compare the analytics with numerical integrations.

2.1. Equations for Calculating the Pulsed Amplitude

We use a spherical coordinate system given by (r, θ, ϕ) for the inertial reference frame of the observer, with its origin at the center of the star. The observer sits at an angle $\theta = 0$. Nonradial oscillations are set in a spherical coordinate system that shares its origin with the observer's coordinates, but is rotated by an inclination angle, i . We denote this by (r, θ', ϕ') , with the pulsation axis, which is coincident with the spin axis, at $\theta' = 0$. The cartesian coordinates of the two frames are related by

$$x' = x \cos i - z \sin i \quad (1a)$$

$$y' = y \quad (1b)$$

$$z' = x \sin i + z \cos i. \quad (1c)$$

Gravitational light bending causes photons that reach the observer to be emitted at an angle $\alpha \geq \theta$, which is given to high accuracy for a Schwarzschild metric by

$$1 - \cos \alpha = (1 - \cos \theta) \left(1 - \frac{r_g}{R}\right), \quad (2)$$

where $r_g = 2GM/c^2$ is the Schwarzschild radius (Beloborodov 2002).

The equations that we derive adopt a number of simplifying assumptions. These are justified because they either are negligible corrections in the context of pulsed emission from a NS, or because they do not affect the energy dependence of the pulsed amplitude. We ignore the effects of frame dragging, which would modify our results by an amount less than the current observational errors (Cadeau et al. 2005 show that a Schwarzschild plus Doppler treatment as presented here provides sufficiently accurate results in comparison to a full relativistic calculation). Lorentz boosting can be ignored since it is a $\lesssim 0.1\%$ correction for a NS spin of $\nu = 600$ Hz, and as well we omit relativistic aberration because it only marginally alters our results. Finally, we also ignore Doppler shifting from

the wave motions because the transverse velocity of r -modes ($\sim 10^7$ cm s $^{-1}$ for an order unity perturbation, approximated from the results of Piro & Bildsten 2005b) is much less than c .

Given these simplifications the observed flux at photon energy E is related to the intensity from the surface, $I(E', \theta', \phi')$, by (Poutanen & Gierliński 2003)

$$F(E) \propto \int \int \delta^3 I(E', \theta', \phi') h(E', \cos \alpha) \cos \alpha d\Omega, \quad (3)$$

where $h(E', \cos \alpha)$ is the limb darkening function, $d\Omega = d \cos \alpha d\phi$ is the angular element, and $E' = E / (\delta \sqrt{1 - r_g/R})$ is the photon energy in a frame co-rotating with the NS surface. The Doppler factor is given by

$$\delta = 1 / (1 - \beta \sin \alpha \sin \phi \sin i), \quad (4)$$

where $\beta = 2\pi R\nu / (c \sqrt{1 - r_g/R})$ is the equatorial velocity (with ν the spin frequency). In addition, equation (3) should have factors due to gravitational redshift, the NS radius, and the NS distance, but we omit these since they cancel when we take the pulsed fraction. The integration limits are $0 \leq \alpha \leq \pi/2$ and $0 \leq \phi \leq 2\pi$.

In general, the limb darkening function can depend on photon energy. This is crucial for studies of ZZ Ceti stars, which have opacities strongly affected by lines, so that the latitudinal quantum numbers can be identified by studying the energy dependence of the pulsed emission (Robinson, Kepler, & Nather 1982; Kepler et al. 2000). In contrast, bursting NSs have a surface opacity dominated by electron scattering. For photons with energy $\gtrsim 1$ keV the limb darkening is largely energy independent and well-approximated by $h = 0.5 + 0.5 \cos \alpha$ (Madej 1991), which is the functional form we assume for our calculations.

Finding the perturbed flux requires perturbing each term in the integrand of equation (3) and keeping terms of linear order. This results in three integrals to evaluate, which correspond to changes in intensity, surface area, and surface normal. Since for nonradial incompressible modes the transverse velocity dominates over the radial velocity ($V_\perp/V_r \sim R/H \gg 1$, where H is the scale height in the bursting layer), the latter two changes are negligible (Buta & Smith 1979; Robinson, Kepler, & Nather 1982). Using just the integral which contains the intensity perturbation, ΔI , the fractional amplitude of the mode is then

$$A(E) \equiv \frac{\Delta F(E)}{F(E)} = \frac{\int \int \delta^3 \Delta I(E', \theta', \phi') h(\cos \alpha) \cos \alpha d\Omega}{\int \int \delta^3 I(E', \theta', \phi') h(\cos \alpha) \cos \alpha d\Omega}. \quad (5)$$

We next relate ΔI to the mode eigenfunction, which is just the temperature perturbation. This relation depends on the bursting NS spectrum, which is well-characterized as a dilute blackbody with a temperature given by a color temperature $T_c \approx (1.4 - 1.6) T_{\text{eff}}$ (Madej 1991; Pavlov, Shibano, & Zavlin 1991; Madej 1997). The change in overall normalization does not affect the energy dependence, hence we use $I(E') = B_{E'}(T_c)$ and perturb this by setting $T_c \rightarrow T_c + \Delta T$, keeping terms of linear order in ΔT ,

$$\frac{\Delta I}{I} = \frac{\partial \log I}{\partial \log T_c} \frac{\Delta T}{T_c} = \frac{x' e^{x'}}{e^{x'} - 1} \frac{\Delta T}{T_c}, \quad (6)$$

where $x' \equiv E'/k_B T_c$. Substituting this result into equation (5), the fractional amplitude becomes

$$A(E) = \frac{\int \int \frac{x' e^{x'}}{e^{x'} - 1} \frac{\Delta T}{T_c}(\theta', \phi') I(E') h(\cos \alpha) \cos \alpha d\Omega}{\int \int I(E') h(\cos \alpha) \cos \alpha d\Omega}, \quad (7)$$

which can be integrated for any angular eigenfunction $\Delta T(\theta', \phi')/T_c$.

2.2. Analytic Estimates

Before we calculate equation (7) numerically we simplify the integrals so that their energy dependence can be studied analytically. There only exists an energy dependence in two terms: $I(E')$ and the logarithmic derivative found in equation (6). If these terms contained no angular dependence, they could be taken outside of the integrals so that the integrals become irrelevant for determining the energy dependence of $A(E)$. In principle this cannot be done because E' contains an angular dependence through the Doppler factor, equation (4), so that the integrals must be performed numerically.

On the other hand, if the Doppler shifts are negligible, then the energy dependence of $A(E)$ is simply

$$A(E) \propto \frac{x' e^{x'}}{e^{x'} - 1}. \quad (8)$$

This has high and low energy limits that are useful for gaining intuition about the expected dependence on energy,

$$A(E) \propto \begin{cases} E/k_B T_c, & E > k_B T_c \sqrt{1 - r_g/R} \\ \text{constant}, & E < k_B T_c \sqrt{1 - r_g/R} \end{cases} \quad (9)$$

At high energies the amplitude is linear with energy, while at low energies the amplitude is approximately constant. This argument shows why a mode will naturally show a larger amplitude at larger energy. *It is simply a result of perturbing a blackbody spectrum, and the fractional change of intensity is much stronger in the Wien tail.* Similar results are found by MOC03 for their hot spot model when the temperature difference between hot and cold regions is small. When the temperature difference they use becomes large, this can lead to deviations away from a linear amplitude-energy relation at high energies ($x' \gtrsim 10$), perhaps providing an important discriminant between the mode and hot spot models. Unfortunately, this is outside the currently observed energy range.

To find the correction to equation (8) introduced by Doppler effects we expand ΔI to first order in $\beta' \equiv \beta \sin \alpha \sin \phi \sin i$, giving

$$\Delta I \approx (\Delta I)_{\beta=0} \left[1 + \beta' \left(\frac{2x' e^{x'}}{e^{x'} - 1} - x' - 1 \right) \right]. \quad (10)$$

When $x' \ll 1$, this changes the amplitude by a factor $1 + \beta'$, which contains no energy dependence. When $x' \gg 1$ the amplitude changes by a factor $1 + \beta' x'$, so that Doppler shifting increases the amplitude at larger energy.

2.3. Comparisons to the Numerical Integrations

We now compare our analytic results to numerical integrations of equation (7). This shows that the analytics reproduce the amplitude versus energy relation. For the angular pattern of the mode, $\Delta T(\theta', \phi')/T_c$, we use a buoyant r -mode with angular quantum numbers $l = 2$ and $m = 1$ (as identified in the

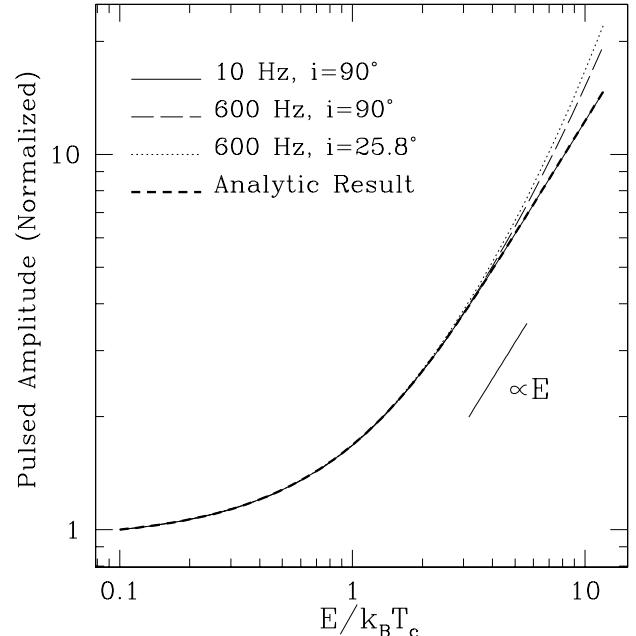


FIG. 1.— The energy dependence of the pulsed amplitude, $A(E)$, for both the full numerical integration and the analytic result given by equation (8) (thick dashed line). The numerical integrations all use a $q = 200$, $l = 2$, $m = 1$ buoyant r -mode on a $M = 1.4 M_\odot$ and $R = 10$ km NS. The parameters we explore are $\nu = 10$ Hz, $i = 90^\circ$ (solid line), $\nu = 600$ Hz, $i = 90^\circ$ (long dashed line), and $\nu = 600$ Hz, $i = 25.8^\circ$ (dotted line). Though the normalization can change drastically for different inclinations (for an example, see Fig. 4 of Heyl 2005) we renormalize all the results to $A(E) = 1$ at $E/k_B T_c = 0.1$ to focus on the shape of the energy dependence. At high energies, $A(E) \propto E$ as we show in §2.2.

slowly rotating limit, Piro & Bildsten 2004), a favored mode for reproducing the frequency evolution of the burst oscillations (Heyl 2004, 2005; Piro & Bildsten 2005b). This mode's latitudinal eigenfunction is parametrized by the spin parameter $q = 2\nu/f$, where f is the mode frequency in a frame co-rotating with the star in units of Hz. A faster spinning NS (higher q) results in an eigenfunction that is more concentrated near the NS equator due to Coriolis effects. We fix $M = 1.4 M_\odot$ and $k_B T_c = 3$ keV so that we can concentrate on whether other attributes of a NS can affect the energy dependence. The amplitude at a given energy is assessed by calculating the time-dependent amplitude and then fitting this with a sinusoidal function.

In Figure 1 we compare integrations of different spins and inclinations, keeping the mode pattern fixed at $q = 200$ as well as fixing M and R . All amplitudes are normalized to $A(E) = 1$ at $E/k_B T_c = 0.1$. At low spin, $\nu = 10$ Hz (solid line), the analytic result of equation (8) (thick dashed line) and the numerical calculation are practically identical. As the spin is increased to $\nu = 600$ Hz (long dashed line) the amplitude increase at high energies, as predicted by equation (10). We also consider a more face-on orientation for the NS ($i = 25.8^\circ$, dotted line), which has the effect of looking like a faster spin NS. This somewhat counterintuitive result has been seen in previous studies (Heyl 2005) and is due the mode pattern, which has a maximum amplitude at latitudes above and below the equator. These comparisons show that neither the spin nor inclination change the energy dependence dramatically from our analytic result.

In Figure 2 we keep the spin and inclination fixed at $\nu =$

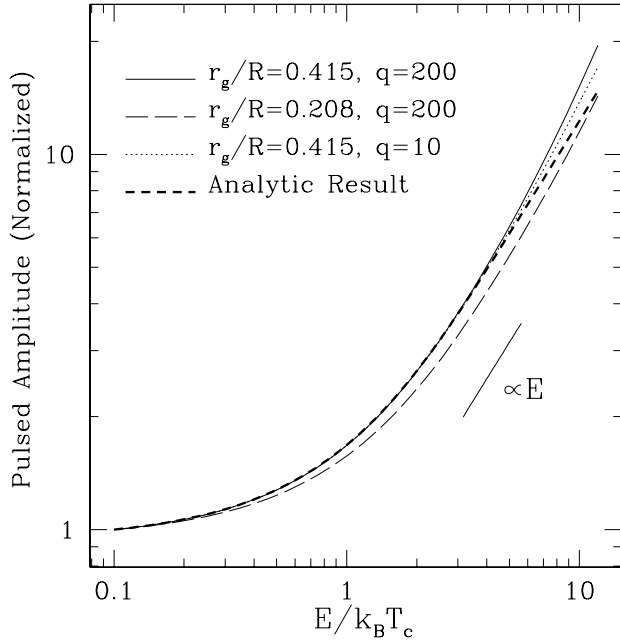


FIG. 2.— The same as Figure 1, but with $\nu = 600$ Hz and $i = 90^\circ$ and varying q and R for the numerical calculations. Setting $R = 20$ km (*long dashed line*) has the effect of decreasing the amplitude at high energies (compare this to the solid line). Decreasing q from 200 to 10 (*dotted line*) affects the energy dependence very little, showing that it is difficult to constrain the surface pattern created by the mode.

600 Hz and $i = 90^\circ$, and investigate the effect of changing q and R . When we set $R = 20$ km (*long dashed line*) the amplitude of the pulsed fraction decreases at high energies. This is because changing R decreases gravitational redshifting so that the break between a constant and linearly increasing amplitude comes at a higher energy (see eq. [9]). We also decrease q dramatically (*dotted line*) but find very little change in the energy dependence. This shows that it is difficult to identify the mode pattern on the NS surface via the amplitude energy dependence.

3. COMPARISONS WITH OBSERVATIONS

MOC03 studied the energy dependence of burst oscillation amplitudes from 6 different bursting NSs. A total of 51 burst oscillation trains were measured, and multiple trains were averaged to obtain amplitude versus energy relations. Some objects were divided into multiple epochs to assure that the gain of the Proportional Counter Array (PCA) on the *Rossi X-Ray Timing Experiment (RXTE)* was relatively constant. To correctly compare our calculations to their results we must weight our pulsed amplitudes by the PCA's effective area, $A_{\text{eff}}(E)$, as well as bin the amplitudes over appropriate energy ranges. The PCA is composed of five Proportional Counter Units (PCUs). Since each of these have approximately the same $A_{\text{eff}}(E)$, we use that of PCU3 for our integrations. The pulsed amplitude is then given by equation (7) with $A_{\text{eff}}(E)$ placed within each integrand. Qualitatively, $A_{\text{eff}}(E)$ has a large wide maximum spread from ≈ 4 –15 keV with a smaller, secondary peak at ≈ 34 keV. The binning of the amplitude depends on the epoch of the observation and is outlined in Table 2 of MOC03.

In Figure 3 we compare the calculated amplitudes with the measurements of MOC03 (*triangles with error bars*). For

the calculated amplitudes we fix $M = 1.4 M_\odot$, $R = 10$ km, $q = 200$, and $i = 90$. The spin is set to the burst oscillation frequency for that object. This is reasonable since in all current mode explanations of burst oscillations the mode moves retrograde with respect to the spin with $\nu \gg f$ (see discussion in Lee & Strohmayer 2005). The normalization of the numerical calculations are set to maximize the fit for each comparison. We consider $k_B T_c = 3$ keV (*solid lines*) as a fiducial temperature exhibited near burst peak. Ideally, we should be able to constrain $k_B T_c \sqrt{1 - r_g/R}$ by fitting for the break in the amplitude (providing M/R if T_c is known). This is difficult because when the photon energy is $\gtrsim k_B T_c$, as is the case for these observations, the amplitude is always linear with energy. Nevertheless, the theoretical calculations show reasonable agreement with the observations.

Comparisons to the observations are complicated by the fact that the observations are averaged over a range of temperatures throughout the cooling of the burst, so that we should consider temperatures in the range of $k_B T_c \approx 2$ –3 keV. If the mode amplitude remains relatively constant, then the pulsed amplitude in the Wien tail should increase as the star cools (see eq.[9]). We test this in Figure 4 for two of the observed amplitudes from Figure 3, but in this case calculating the amplitudes for temperatures of $k_B T_c = 2$ keV (*dashed lines*) and 3 keV (*solid lines*). The overall normalization is chosen to maximize the fit, but the relative amplitude of the two curves in each panel is set by the temperature ratio. The two temperatures envelop the data, showing that the spread in the data may be due to cooling in the burst tail. An interesting future test of our work would be to divide the burst data into early and late stages, and see whether the amplitude evolves. This expected temperature dependence can be divided out of the data to investigate how much the amplitude of the mode is changing due to other effects (e.g., changes in the intrinsic amplitude, or changes in q).

4. OPTIMAL ENERGIES FOR DETECTION OF NEUTRON STAR MODES

Since we understand the spectrum of the burst oscillations, this can be used to find the optimal photon energy range for burst oscillations searches. The pulsed signal is given by the total number of pulsed photons integrated over some energy range,

$$S = \sqrt{1 - \frac{r_g}{R}} \left(\frac{R}{D} \right)^2 t_{\text{obs}} \int A_{\text{eff}}(E) \frac{dE}{E} \times \int \int \frac{x' e^{x'}}{e^{x'} - 1} \frac{\Delta T}{T_c} I(E') h(\cos \alpha) \cos \alpha d\Omega, \quad (11)$$

where D is the source distance, t_{obs} is the observing time, and we have assumed $\delta \approx 1$. The background noise within this energy range is estimated from photon counting statistics

$$N = \left[\sqrt{1 - \frac{r_g}{R}} \left(\frac{R}{D} \right)^2 t_{\text{obs}} \int A_{\text{eff}}(E) \frac{dE}{E} \times \int \int I(E') h(\cos \alpha) \cos \alpha d\Omega \right]^{1/2}, \quad (12)$$

which is the square-root of the total number of photons detected,

To evaluate equations (11) and (12) we use a blackbody spectrum, $I(E') = B_{E'}(T_c)$, with $k_B T_c = 3$ keV, and the analytic pulsed fraction, ignoring Doppler corrections, since the agreement is so close between the numerical and analytic results.

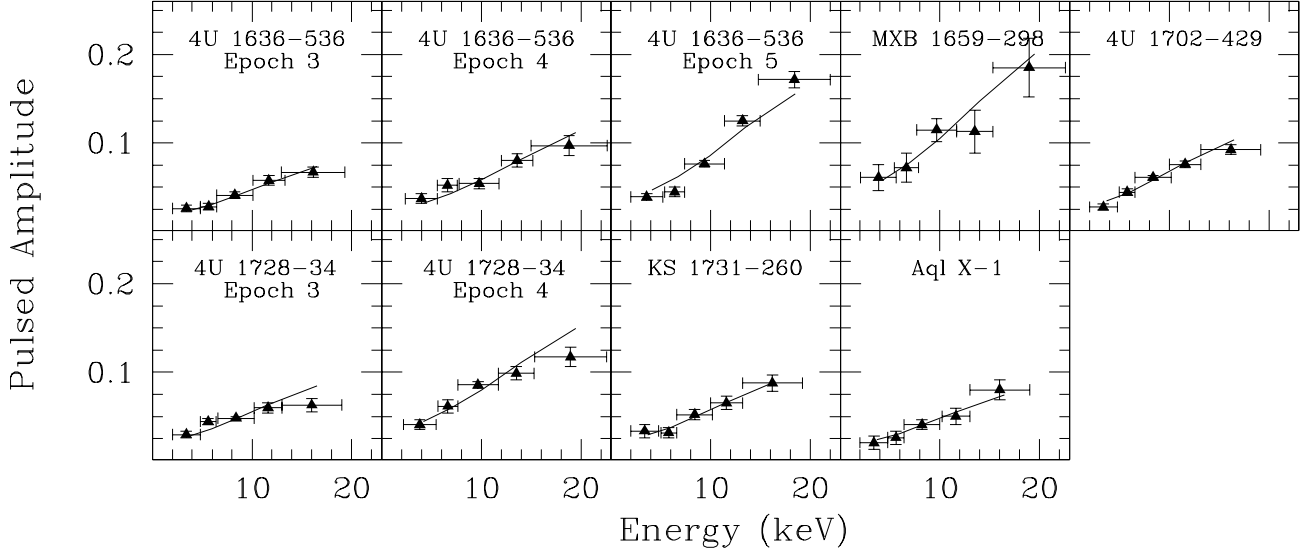


FIG. 3.— The observed energy dependence of the burst oscillation amplitudes (MOC03, *triangles with error bars*), in comparison with our full numerical calculations using $k_B T_c = 3$ keV (*solid lines*). We label each panel with the NSs name and the epoch of the measurements if that NS was observed over multiple epochs. For each calculation the spin is set to that object’s burst oscillation frequency and the normalization is set to maximize the fit.

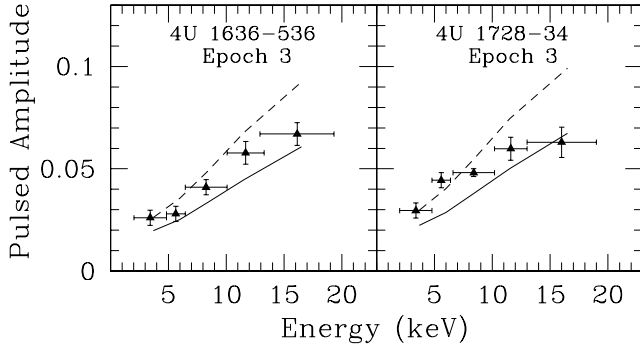


FIG. 4.— The observed energy dependence of the burst oscillations amplitudes (MOC03, *triangles with error bars*), for 2 of the 9 panels from Fig. 3. These represent a relatively “good” fit (*left panel*) and a “poor” fit (*right panel*). We compare these with our numerical calculations using $k_B T_c = 2$ keV (*dashed lines*) and 3 keV (*solid lines*). The overall normalization is set to maximize the fit with the data, but the relative amplitude of the two curves is set by the two temperatures. This shows that the observed spread in that data could arise from the cooling of the NS in the burst tail.

We assume $D = 4.3$ kpc (using 4U 1728–30 for a fiducial distance), $t_{\text{obs}} = 10$ s (one X-ray burst) and $\Delta T/T_c = 0.025$ (which replicates the observed pulsed fractions). In Figure 5 we plot these S/N calculations using three different forms for A_{eff} : a flat energy response with $A_{\text{eff}} = 1000$ cm² (*solid line*), the A_{eff} of one PCU from *RXTE*’s PCA (*dotted line*), and the proposed A_{eff} for the *Nuclear Spectroscopic Telescope Array* (*NuSTAR*; Harrison et al. 2004, *dashed line*), a future X-ray mission. For each we show a series of 3 keV integrations, which are then connected with lines to guide the eye. This comparison demonstrates that the energy range of ≈ 2 –25 keV contributes most to S/N . Other than integrating over this range, there is little more an observer can do to maximize the opportunity of finding burst oscillations. At high energies the pulsed fraction

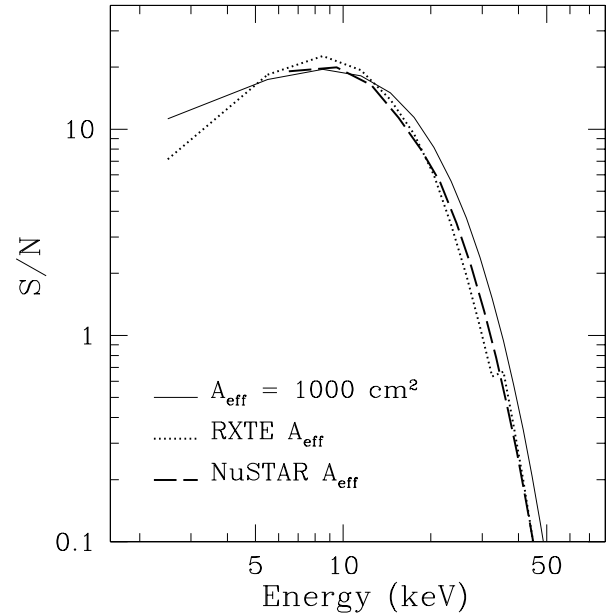


FIG. 5.— The ratio of signal to noise (using eqs. [11] and [12]) expected for a NS surface mode during a 10 s X-ray burst. We set $k_B T_c = 3$ keV, $D = 4.3$ kpc, and $\Delta T/T_c = 0.025$, and compare a flat energy response (*solid line*), the $A_{\text{eff}}(E)$ of one PCU on *RXTE*’s PCA (*dotted line*), and the proposed A_{eff} for the *NuSTAR* mission (*dashed line*). Each curve connects a series of points, with each point representing an integration over a 3 keV width energy bin.

is considerably higher, but this range is not necessarily better since there are so few photons in the Wien tail and because A_{eff} drops at higher energies. Future missions interested in burst oscillations searches could mitigate this by having large A_{eff} at higher energies.

It is especially exciting that *NuSTAR* may be able to ob-

serve burst oscillations. Though *NuSTAR*'s specifications of a large A_{eff} , high energy range ($\approx 5 - 80$ keV), and good spectral resolution (900 eV at 68 keV) are tuned for observations of black holes, active galactic nuclei, and supernova remnants, it also has fast timing (~ 1 ms) which makes it ideal for studying burst oscillations. In addition, its high angular resolution (≈ 40 arcsec) coupled with its timing abilities may make it useful for identifying accreting millisecond pulsars in crowded fields such as at the Galactic center (something beyond *RXTE*'s capabilities). A typical accreting millisecond pulsar at the galactic center has a peak flux in outburst 100 times less than a type I burst, so the persistent pulse could easily be found in a ≈ 1 day long observation.

5. DISCUSSION AND CONCLUSIONS

We have studied the energy dependence of NS surface mode amplitudes for NS surface temperatures of $k_B T_c = 3$ keV and compared this with burst oscillations. The observations follow our calculated trend of a linear amplitude for photon energies $\gtrsim k_B T_c$ and becoming flatter when the photon energy is $\approx k_B T_c$. Unfortunately, there are currently no data for burst oscillations below an energy of $k_B T_c$. Measuring the amplitude at such an energy is crucial for fully testing the mode explanation of burst oscillations. One must be cautious of interpretations for $E' \lesssim 1$ keV because limb darkening begins to depend on energy in this range, so that equation (8) is no longer applicable. However, this also raises the possibility for surface pattern identification at low energies (analogous to what is done for pulsating WDs, Kepler et al. 2000).

The agreement between our analytic result and the observations is promising for explaining burst oscillations as modes, but frustrates the ability of using burst oscillations as a tool to learn about these NSs. As long as the amplitude of the surface perturbation caused by the mode is unknown, it will be difficult to constrain NS properties. Future theoretical studies should work to address this unanswered question. We expect all bursting NS modes to show the energy dependence we present here, including the oscillation seen in the 4U 1636–53 superburst (Strohmayer & Markwardt 2002), for which this energy dependence was not determined.

However, other types of NS pulsations need not match this, for example millisecond accreting pulsars in their persistent emission. This raises the critical question of what is the energy dependence of the burst oscillations from these systems (SAX J1808.4–3658 [Chakrabarty et al. 2003] and

XTE J1814–338 [Strohmayer et al. 2003]). Piro & Bildsten (2005b) describe a number of differences between the properties of burst oscillations from pulsars and nonpulsars. These differences may simply be due to deviations in magnetic field strength, but they could instead indicate that the pulsar burst oscillations are due to a completely different mechanism. Measuring their energy dependence would help to settle this unresolved issue.

One topic we have not addressed is the phase lag observed for high energy photons in burst oscillations (MOC03). We focused on the amplitude relation because of its stronger statistical evidence in the observations. For individual oscillation trains measured by MOC03, only 13 out of 51 exhibit phases that vary as a function of energy at 90% confidence. In comparison, 34 of these exhibit some dependence with energy at 90% confidence (with the remaining typically having less counts in their folded profile). Nevertheless, it is somewhat troubling that our calculations find the reverse phase dependence due to Doppler shifts, just as was found in previous studies of pulsed emission from NSs (e.g., Weinberg, Miller, & Lamb 2001; Heyl 2005). This inconsistency has been cited by many as evidence that a Comptonizing corona exists around a NS during an X-ray burst. Without further theoretical studies of the physical limits of such a Comptonizing corona or further investigations on how robust of a property this observed hard phase lag is, it is not presently clear how dire this inconsistency is for the mode explanation of burst oscillations. Lee & Strohmayer (2005) have found some parameter space in R and i that exhibit hard lags, which may be promising to pursue further. Though their result is for a different eigenfunction than we consider here, it does not affect our main conclusions since the energy dependence will still be independent of the specific mode.

We appreciate the help of Mike Muno for providing us with the pulsed amplitude data and Philip Chang for reading and contributing comments on a previous draft. We thank Fiona Harrison for providing us with the effective area response of the *NuSTAR* satellite. We also thank Deepto Chakrabarty and Andrew Cumming for many helpful discussions. This work was supported by the National Science Foundation under grants PHY99-07949 and AST02-05956, and by the Joint Institute for Nuclear Astrophysics through NSF grant PHY02-16783.

REFERENCES

- Beloborodov, A. M. 2002, *ApJ*, 566, L85
 Bildsten, L. 1995, *ApJ*, 438, 852
 Bildsten, L. 1998, in *The Many Faces of Neutron Stars*, ed. R. Buccheri, J. van Paradijs & A. Alpar (Dordrecht: Kluwer), 419
 Buta, R. J. & Smith, M. A. 1979, *ApJ*, 232, 213
 Cadeau, C. Leahy, D. A., & Morsink, S. M. 2005, *ApJ*, 618, 451
 Chakrabarty, D., Morgan, E. H., Muno, M. P., Galloway, D. K., Wijnands, R., van der Klis, M., & Markwardt, C. B. 2003, *Nature*, 424, 42
 Cui, W., Morgan, E. H., & Titarchuk, L. G. 1998, *ApJ*, 504, L27
 Galloway, D. K., Chakrabarty, D., Morgan, E. H., & Remillard, R. A. 2002, *ApJ*, 576, L137
 Harrison, F., *NuSTAR* Science Team, 2004, HEAD, 8,4105
 Heyl, J. S. 2004, *ApJ*, 600, 939
 Heyl, J. S. 2005, *MNRAS*, 361, 504
 Kepler, S. O., Robinson, E. L., Koester, D., Clemens, J. C., Nather, R. E., & Jiang, X. J. 2000, *ApJ*, 539, 379
 Lee, U. 2004, *ApJ*, 600, 914
 Lee, U. & Strohmayer, T. E. 2005, *MNRAS*, 361, 659
 Madej, J. 1991, *ApJ*, 376, 161
 Madej, J. 1997, *ApJ*, 320, 177
 Muno, M. P., Chakrabarty, D., Galloway, D. K., & Psaltis, D. 2002, *ApJ*, 580, 1048
 Muno, M. P., Chakrabarty, D., Galloway, D. K., & Savov, P. 2001, *ApJ*, 553, L157
 Muno, M. P., Özel, F., & Chakrabarty, D. 2002, *ApJ*, 581, 550
 Muno, M. P., Özel, F., & Chakrabarty, D. 2003, *ApJ*, 595, 1066 (MOC03)
 Page, D. 1995, *ApJ*, 442, 272
 Pavlov, G. G., Shibano, Y. A., & Zavlin, V. E. 1991, *MNRAS*, 253, 193
 Piro, A. L. & Bildsten, L. 2004, *ApJ*, 603, 252
 Piro, A. L. & Bildsten, L. 2005a, *ApJ*, 619, 1054
 Piro, A. L. & Bildsten, L. 2005b, *ApJ*, 629, 438
 Poutanen, J. & Gierliński, M. 2003, *MNRAS*, 343, 1301
 Robinson, E. L., Kepler, S. O., & Nather, R. E. 1982, *ApJ*, 259, 219
 Spitkovsky, A., Levin, Y., & Ushomirsky, G. 2002, *ApJ*, 566, 1018
 Strohmayer, T. E. & Bildsten, L. 2003, in *Compact Stellar X-Ray Sources*, ed. W. H. G. Lewin & M. van der Klis (Cambridge: Cambridge Univ. Press), in press (astro-ph/0301544)
 Strohmayer, T. E. & Markwardt, C. B. 2002, *ApJ*, 577, 337
 Strohmayer, T. E., Markwardt, C. B., Swank, J. H., & in 't Zand, J. 2003, *ApJ*, 596, L67
 Weinberg, N., Miller, M. C., & Lamb, D. Q. 2001, *ApJ*, 546, 1098